Theoretical investigation of polarization control in ultraviolet wavelength region using eigenmode within subwavelength grating

Yuusuke Takashima[1,3]*, Masato Tanabe[1], Masanobu Haraguchi[1,2], Yoshiki Naoi[1,2]

[1] Graduate School of Advanced Technology and Science, Tokushima University, 2-1 Minami-josanjima, Tokushima 770-8506, Japan

[2] Graduate School of Science and Technology, Tokushima University, 2-1 Minami-josanjima, Tokushima 770-8506, Japan

[3] Research Fellow of Japan Society for the Promotion of Science

*E-mail address: takashima@ee.tokushima-u.ac.jp, Phone: +81 88 656 7447.

Abstract

The optical characteristics of a subwavelength grating (SWG) were examined as a means of achieving ultraviolet (UV) polarization control based on the interaction between a light wave and Bloch eigenmode wave in the SWG, which results in a spatial periodic refractive index distribution. The relation of dispersion of the eigenmode wavevector was calculated to reveal the light propagation mechanism in this structure. The expected optical characteristics proved the feasibility of obtaining highly polarized UV light with no significant decrease in light intensity. The effects of the higher-order eigenmode on the SWG optical characteristics were also examined and discussed via the finite-difference time-domain method. This approach provides new insight into the SWG design for UV polarization control using the above interaction.

Keywords: subwavelength, polarization, ultraviolet, eigenmode, grating

1. Introduction

Highly polarized ultraviolet (UV) light is suitable for unique applications. For example, highly polarized UV irradiation induces optical anisotropy in reactive polymers, which are favorable for photo-alignment devices. Note that irradiation with visible light does not yield the same effects [1, 2]. This property of UV light is favorable for achieving liquid crystal alignment without the use of rubbing and patternable processes. A UV polarization control method that does not cause a dramatic decrease in the light intensity is required for remarkable achievements of highly polarized UV light applications.

Currently, dichromatic polarizing plates composed of iodine-doped polymers are widely used to generate polarized UV light. A high polarization ratio is obtained using this filter; however, the transmittance of the filter is very low owing to the doped iodine polymer. A subwavelength grating (SWG), which has a shorter period than the incident wavelength λ, is a candidate to overcome this issue [3–24]. In this structure, a Bloch eigenmode wave exists for each orthogonal polarization state, which is caused by the periodic refractive index n_{bar} distribution. This eigenmode wave interacts with the incident light wave under certain conditions [3, 12, 13, 16, 17, 19, 20–24]. Utilizing these interactions, high polarization selectivity is achieved without a significant decrease in the transmitted light intensity.

Traditionally, the SWG electromagnetic response has been examined using effective medium theory (EMT) [5, 7, 15, 20]. In EMT, one assumes that only a fundamental eigenmode wave with a certain propagation constant exists in the SWG structure. In other words, the SWG structure is approximated as a uniform layer with an effective

refractive index value. However, the EMT-predicted optical characteristics of the SWG are only accurate if the grating period Λ is significantly shorter than λ [5, 20]. As Λ approaches λ, the actual electromagnetic response in the SWG deviates from that predicted using the EMT. The origin of this deviation is the energy propagation by several eigenmodes within the SWG structure. Recently, the SWG optical characteristics incorporating multiple eigenmodes have been theoretically examined in the infrared (IR) wavelength region [20–24]. This analysis was performed for an SWG with a real n_{bar} only, because the imaginary part of the material n_{bar} is negligible in the IR wavelength region. However, the imaginary part of the SWG n_{bar} in the UV wavelength region is larger than that in the IR region. Thus, the effect of the imaginary part on the eigenmode state in the SWG is not negligible in the UV region, and the optical characteristics in that region deviate from those in the IR region. In order to design an SWG for polarization control in the UV region, the eigenmode is determined with consideration of the effect of the n_{bar} imaginary component on the eigenmode state.

In this study, the optical characteristics of the SWG are theoretically examined in the UV region. The complex dispersion relation of the eigenmode wavevector is examined in order to elucidate the light propagation mechanism in the SWG. Further, the distribution of electromagnetic field within the SWG is calculated using a finite difference time domain (FDTD) method, in order to interpret and discuss the physical characteristics of the eigenmode within the SWG structure, and the new insight of the SWG design for UV polarization control is presented, based on theoretical considerations of the eigenmode.

2. Complex Dispersion Relation Analysis

The interaction between the Bloch eigenmode and the incident light dominates the electromagnetic response in the SWG structure. On the basis of the dispersion relation of the eigenmode wavevector, we examined the light propagation mechanism in the UV region to elucidate and examine the SWG optical characteristics. Figure 1 shows a cross-sectional view of the SWG structure used for the dispersion analysis. In this figure, the SWG structure was arranged in air. Normal incident light was assumed, with a monochromatic plane wave having $\lambda = 365$ nm, which was s- or p-polarized. In the case of s-polarization, the electric-field vector was parallel to the grating stripe; it was perpendicular for p-polarization. The symbols H, s, and a defined in Fig. 1 indicate the grating height, grating width, and air-gap width, respectively. In previous studies, Λ and the filling factor (defined as the ratio of s to Λ) were related to the Bloch eigenmode order and were set to $\Lambda = \lambda/3.6$ and $s/\Lambda = 0.5$, respectively, to yield high polarization selectivity [16, 17, 19, 22]. The grating was assumed to have an infinite length in the y-direction, because the actual grating length in the y-direction is significantly larger than λ.

Four grating materials were assumed: Si, Ge, Pt, and Cr, which have various n_{bar} values. Subsequently, the effects of the real and imaginary parts of each material n_{bar} on the SWG optical characteristics were examined. The n_{bar} values at $\lambda = 365$ nm for Si (6.5271 + 2.6672i), Ge (4.0716 + 2.576i), Cr (1.8636 + 2.6793i), and Pt (1.64 + 2.64i) are obtained from previous studies [25–27].

Within the SWG region, the eigenmode amplitude in the lateral direction (x-direction) was modulated by the periodic n_{bar} distribution, as detailed in Ref. [22]. The symbols k_a and k_s in Fig. 1 are the lateral wavenumber vectors of the eigenmode in the air-gap and in the highly refractive region of the grating, respectively. In the z-direction, the light wave propagated as a plane wave with propagation constant β. In this model, the relation of dispersion between k_a and k_s is obtained by considering the continuity of the electromagnetic field in the SWG. The relation of dispersion for the p-polarization is [22]

$$n_{bar}^{-2} k_{s,m} \tan(k_{s,m} s/2) = -k_{a,m} \tan(k_{a,m} a/2) \quad (m = 1, 2, 3\cdots), \tag{1}$$

where m is the number of the eigenmode order.

The relationship between k_s or k_a and β_m is

$$\left(\frac{2\pi}{\lambda}\right)^2 - k_{a,m}^2 = \left(\frac{2\pi n_{bar}}{\lambda}\right)^2 - k_{s,m}^2 = \beta_m^2 \quad (m = 1, 2, 3\cdots). \tag{2}$$

For the dispersion relation of s-polarization, the n_{bar} term in Eq. (1) is replaced with 1 [22]. The solutions of Eq. (1) indicate that the energy of the incident light wave can be transferred to the eigenmode wave. Further, the solutions in ascending order correspond to m. For example, the first solution of Eq. (1) corresponds to the first-order eigenmode

(m = 1).

Note that some of the eigenmode energy disappears upon light propagation in the SWG, provided the SWG material has a light absorption capability. In this case, the eigenmode possesses complex lateral and vertical wave vectors. Hence, we expanded k_a, k_s, and β_m to complex numbers in order to reveal the light propagation mechanism in the SWG, because the light absorption cannot be neglected in the UV wavelength region.

Figure 2 shows the real and the imaginary values of β_m obtained by solving Eq. (1), for the various examined materials. When β is a complex number, the eigenmode propagates along the z-direction with the decay of the light intensity, and we cannot precisely distinguish the propagation and evanescent mode. We considered up to second-order eigenmode (m = 2), because the amplitude of more higher-order eigenmodes rapidly decrease and typically became very low [22]. The solid and dashed lines correspond to the first- and second-order eigenmodes, respectively. When only the real or the imaginary part of Eq. (1) was satisfied, we consider the eigenmode can possess the wavenumber vector according to the following rationale. The real and imaginary parts of Eq. (1) indicate the phase matching and the decreasing of the amplitude matching condition, respectively. When the grating has a light absorption capability, the energy of the incident light dissipates into the grating material. This decreases the eigenmode lifetime, and the amplitude and the phase of the mode cannot be determined simultaneously. The uncertainty between the amplitude and the phase broadens the eigenmode states, which leads to the relaxation of the resonance condition. Thus, the mode can possess the complex wave number, which satisfies only the real or

the imaginary part of Eq. (1).

For p-polarization, the dispersion relation indicates that the absolute values of the imaginary parts of the first- and second-mode propagation constants, namely, the propagation loss, are lower for a high-refractive-index SWG (with Si or Ge, labeled Si- or Ge-SWG, respectively) than that for a low-refractive-index SWG (the Pt- or Cr-SWG), as shown in Fig. 2(a). In general, the imaginary part of the material n_{bar} is directly related to the light absorption in the material. This causes energy loss of the incident wave, and this loss generally increases as the absolute value of the imaginary part of the n_{bar} is increased. As a result, the propagation loss and the value of the n_{bar} imaginary component are mutually related.

In contrast, the result shown in Fig. 2(a) indicates that the absorption coefficient is not directly related to the propagation loss, and the propagation loss in the high-refractive-index SWGs can become lower than that in the low-refractive-index SWGs in spite of the large absorption coefficient. The reason for this behavior is explained as follows. The eigenmode is defined as a solution of Maxwell's equations for the periodic n_{bar} distribution, and the eigenmode must satisfy the electromagnetic boundary condition inside the SWG structure. The eigenmode state and the excitation conditions are strongly dependent on the geometric shape. Therefore, the propagation loss in the SWG is not only determined by the material properties, but also by the geometry. According to the dispersion analysis result, the eigenmodes within the Ge- and Si-SWGs are tuned to yield high p-polarization transmittance by controlling the SWG geometry, despite the large absorption coefficient. These types of SWGs are,

therefore, suitable for maintaining high transmittance throughout the structure.

We also obtained solutions to Eq. (1) for an s-polarized incident wave, as shown in Fig. 2(b). This figure shows that the s-polarization propagation loss is significantly larger than that of the p-polarization case for all examined gratings. The s-polarization transmittance through the Si- and Ge-SWGs is lower than that through the Pt- and Cr-SWGs, because the absolute value of the imaginary part of the first-order mode propagation constant in the Si- and Ge-SWG is larger than that for the other gratings. The difference in the eigenmode characteristics between the p- and s-polarization are attributed to the difference in the electric field direction between the two orthogonal polarization states, because the eigenmode state is strongly dependent on the boundary condition and the structure geometry for the electric field of the light. As a result, the dispersion relation suggests that a high-refractive-index material is suitable for achieving high polarization selectivity and high transmittance in the UV wavelength region.

3. FDTD Calculation Results and Discussion

To evaluate the actual optical characteristics of the SWG, the electromagnetic field distribution was calculated using the FDTD method. The calculation model is shown in Fig. 3, where the calculation region is defined as the square region surrounded by broken lines. The vertical and lateral sizes of the calculation region were 715 nm and 405 nm, respectively. A perfectly matched layer (PML) and periodic boundary condition (PBC) were employed as the boundary conditions for the *z*- and *x*-directions,

respectively. There were 20 PML layers, and the calculation region was divided into a 2 nm × 2 nm rectangular cell. The calculation time step was 3.3×10^{-18} s. In the model, an SWG structure was arranged in air. A p- or s-polarized incident plane wave with λ = 365 nm was propagated through the SWG, and the transmittance through the SWG was calculated at the observation plane, as shown in Fig. 3.

Figure 4 shows the calculated transmittance through the SWG structure as a function of H. Note that the transmittance converges to 100% at H = 0. The reason is explained as follows. In the case of H = 0, the light propagates in free space. On the other hand, the eigenmode due to the SWG starts propagating energy with increasing H. Therefore, the transmittance varies rapidly around H = 0. The transmittance of p-polarization was significantly larger than that of the s-polarization for all SWG cases and oscillated with increased H. In the region up to H = 30 nm, the transmittance through the Si- and Ge-SWGs was higher than that through the low-refractive-index SWGs. In the region of H = 50–100 nm, the transmittance through the high-refractive-index SWGs was lower than that through the low-refractive-index SWGs. On the other hand, the electromagnetic response for the s-polarization varied significantly from that for the p-polarization case. That is, the s-polarization transmittance significantly and monotonically decreased with increased H, and became significantly smaller than that obtained for the p-polarization case.

Overall, the polarization ratio (defined as the transmittance ratio of the p- to s-polarization) increases with increasing H, and the Si-SWG polarization ratio is the highest of all the examined gratings, at more than 9×10^4 for H = 100 nm, while

maintaining ~40% transmittance. These results suggest that both high polarization selectivity and high transmittance can be achieved in the UV wavelength region using a Si-SWG. The tendency of the optical characteristics determined via the FDTD method agrees with that obtained by considering the dispersion relation. Moreover, the magnetic field distribution in the Ge-SWG at H = 100 nm is shown in Fig. 5. The field distribution was normalized by the field intensity of the light source. The black region indicates a high field intensity, namely a saturated field intensity. Figure 5 reveals that the distribution obtained when the imaginary part of the SWG n_{bar} is considered varies significantly from that obtained when the imaginary part is neglected. Further, these FDTD calculation results are significantly different from the optical characteristics of the SWG predicted via EMT. Consequently, consideration of the eigenmode is essential for the evaluation of the SWG optical characteristics.

In order to interpret and discuss the physical characteristics of the eigenmode, the FDTD calculation results were compared with those yielded by the dispersion relation. For p-polarization, the FDTD calculation results indicate good agreement with the prediction of dispersion relation in the region up to H = 30 nm. For H = 50–100 nm, however, the transmittance through the Pt- and Cr-SWGs is higher than that through the Si- and Ge-SWGs, which is contrary to the prediction of dispersion relation. Considering the s-polarization, the transmittance through the Ge-SWG is higher than that for the Si-SWG. Moreover, this result disagrees with the prediction of dispersion relation. These discrepancies occur only for the high-refractive-index SWGs.

In order to elucidate the origin of this disagreement, the dependence of the p-polarized

eigenmode magnetic field distribution in the Ge-SWG on H was determined, as shown in Fig. 6. This SWG was selected because it exhibits significant variation in the transmittance of p-polarization with increasing H. The green-squares in Fig. 6 indicate the highly refractive region of the grating. In Fig. 6, the field intensity of the blue region in the green-squares increased with increasing H, whereas the red region remained almost unchanged. This indicates that the field distribution of the eigenmode varied with increasing H. Therefore, one of the origins of the above discrepancies is attributed to the transformation of the incident light energy into the higher-order eigenmode, because the energy transformation into the higher-order mode in a high-refractive-index SWG can become larger than that in the low-refractive-index SWG [3, 12, 13, 22]. We consider up to the second higher order mode, because the higher order mode than the second significantly decreases with propagation. To confirm the effect of the higher-order mode on the SWG optical characteristics, we examined the transmittance through the Ge-SWG for various weightings of the first- and second-order eigenmodes. The transmittance was evaluated by the electric field of the first- and second-order eigenmodes and the ratio of the incident light intensity to the transmitted intensity was determined. To examine the dependence of the transmittance decay on the ratio of each mode weight, we considered only the imaginary part of β. Moreover, the difference of the real part of β causes the phase difference between the eigenmodes when the modes pass through the SWG. The difference of the phase influences on the transmittance through the SWG. This effect of the real part of β on the mode phase was considered for calculating the mode weight.

The first- and second-order modes with the imaginary components $\beta_1\Lambda = -0.4709$ and $\beta_2\Lambda = -6.014$ were used for the investigation, with the above values being obtained from the relation of dispersion. The envelope of the total electromagnetic field within the SWG was expressed in terms of the superposition of the excited modes, i.e., $A_1\exp(-0.4709H/\Lambda) + A_2\exp(-6.014H/\Lambda)$, where A_1 and A_2 are the first- and second-order mode weights, respectively.

Figure 7 shows the dependence of the transmittance through the Ge-SWG as a function of H for various first- and second-order mode weights. This figure demonstrates that the optical characteristics agree with those yielded by the FDTD calculation when the weights of the first- and second-order eigenmodes are adjusted with increasing H. This agreement is explained by considering the modulation of n_{bar} with increasing H. As Si- and Ge-SWGs have higher n_{bar} values than the other examined substances, the degree of the n_{bar} modulation for these materials increases with increased H. The oscillator strength of each mode is modified by the variety of the n_{bar} modulation, and the transformation of the light energy into the higher-order mode is changed. Thus, the weight of each eigenmode varies with increasing H. The propagation loss for the higher-order modes is larger than that for the lower-order mode. As a result, the transmittance through the SWG is influenced by the changes in the transformation of photon energy into higher-order eigenmode. By referring previous studies, we verified the estimated weight of each mode [28]. The weight was calculated by

$$A_{n,m} = \frac{\int_0^{\Lambda} \left| h_{y,m}^{in}(x) \right|^2 dx}{\left| \int_0^{\Lambda} \frac{1}{r^2(x)} h_{y,n}^{out}(x) h_{y,m}^{in}(x) dx \right|} \quad (3)$$

The symbol *r(x)* denotes the refractive index and 1 in air-gap of the SWG. In the grating bar, the *r(x)* is n_{bar}, where n = 0, 1, 2… denote the diffraction order outside the SWG. In the SWG, only the 0^{th} diffraction (n = 0) propagates the energy of the light. *r(x)* is the refractive index of the medium. The symbols $h_{y,n}^{out}(x)$ and $h_{y,n}^{in}(x)$ are lateral magnetic fields of the profile inside and outside the SWG and are obtained from previous studies [22]. The calculated mode weights of first and second were about 9.55 and 0.45, respectively. These calculated mode weights agree with our estimated mode weights.

4 Conclusion

The optical characteristics of various SWGs in the UV region have been examined. The complex dispersion relation was employed in order to elucidate the light propagation mechanism, and the optical characteristics in the UV wavelength region were examined. Moreover, the effect of the complex n_{bar} value on the optical characteristics of the SWG was investigated. The results indicate that a high-refractive-index SWG is suitable for achieving both high polarization selectivity and high transmittance. Furthermore, the electromagnetic field distribution was calculated using the FDTD method to interpret the physical characteristics of the

eigenmode within the SWG structure and to discuss the predicted optical characteristics. The FDTD calculation results show good agreement with those predicted by the dispersion relation, provided the effects of the higher-order eigenmode are considered. The results indicate that the eigenmodes in the Si- and Ge-SWGs are suitable for UV polarization control. In particular, the Si-SWG polarization ratio reached 9×10^4 while maintaining approximately 40% p-polarization transmittance. These results indicate that both high polarization and high transmittance are achieved. These findings provide new insights on SWG design for UV polarization control and can play an important role in the development of UV polarization control devices.

Acknowledgment

We thank Dr. T. Tomita of Tokushima University for discussing the calculation results.

Reference list

1. Watanabe, H., Miyagawa, N., Takashra, S., Yamaoka, T.: Photo-alignment material with azobenzene-functionalized polymer linked in film. Polym. Adv. Technol. **13**, 558-565 (2002)

2. Choi, D.H., Cha, Y.K.: Photo-alignment of low-molecular mass nematic liquid crystals on photoreactive polyimide and polymethacrylate film by irradiation of a linearly polarized UV light. Polym. Bull. **48**, 373-380 (2002)

3. Chou, S.Y., Deng, W.: Subwavelength amorphous silicon transmission gratings and applications in polarizers and waveplate. Appl. Phys. Lett. **67**, 742-744 (1995)

4. Zhuang, L., Schablitsky, S., Shi, R.C., Chou, S.Y.: Fabrication and performance of thin amorphous Si subwavelength transmission grating for controlling vertical cavity surface emitting laser polarization. J. Vac. Sci. Technol. B **14**, 4055-4057 (1996)

5. Yu, X.J., Kwok, H. S.: Optical wire-grid polarizers at oblique angles of incidence.: J. Appl. Phys. **93**, 4407-4412 (2003)

6. Yang, Z.Y., Lu, Y.F.: Broadband nanowire-grid polarizers in ultraviolet-visible-near-infrared regions.: Opt. Express **15**, 9510-9519 (2007)

7. Lee, J.H., Song, Y.W., Lee, J.G., Ha, J., Hwang, K.H., Zang, D.S.: Optically bifacial thin-film wire-grid polarizers with nano-patterns of a graded metal-dielectric composite layer.: Opt. Express **16**, 16867-16876 (2008)

8. Weber, T., Kasebier, T., Szeghalmi, A., Knez, M., Kley, E.B., Tunnermann, A.: Iridium wire grid polarizer fabricated using atomic layer deposition.: Nanoscale Res. Lett. **6**, 558 (2011)

9. Weber, T., Kasebier, T., Helgert, M., Kley, E.B., Tunnermann, A.: Tungsten wire grid polarizer for applications in the DUV spectral range. Appl. Opt. **51**, 3224-3227 (2012)

10. Asano, K., Yokoyama, S., Kemmochi, A., Yatagai, T.: Fabrication and characterization of a deep ultraviolet wire grid polarizer with a chromium-oxide subwavelength grating. Appl. Opt. **53**, 2942-2948 (2014)

11. Weber, T., Kroker, S., Kasebier, T., Kley, E.B., Tunnermann, A.: Silicon wire grid polarizer for ultraviolet applications. Appl. Opt. **53**, 8140-8144 (2014)

12. Chang-Hasnain, C.J.: High-contrast grating as a new platform for integrated optoelectronics. Semicond. Sci. Technol. **26**, 014043 (2011)

13. Chang-Hasnain, C.J., Yang, W.: High-contrast grating for integrated optoelectronics. Adv. Opt. Photonics **4**, 381-440 (2012)

14. Wu, T.T., Syu, Y.C., Wu, S.H., Chen, W.T., Lu, T.C., Wang, S.C., Chiang, H.P., Tsai, D.P.: Sub-wavelength GaN-based membrane high contrast grating reflector. Opt. Express **20**, 20551-20557 (2012)
15. Zhang, L., Teng, J.H., Chua, S.J., Fitzgerald, E.A.: Linearly polarized light emission from InGaN light emitting diode with subwavelength metallic nanograting. Appl. Phys. Lett. **95**, 261110 (2009)
16. Ma, M., Meyaard, D.S., Shan, Q., Cho, J., Schubert, E.F., Kim, G.B., Kim, M.H., Sone, C.: Polarized light emission from GaInN light-emitting diodes embedded with subwavelength aluminum wire-grid polarizers. Appl. Phys. Lett. **101**, 061103 (2012)
17. Takashima, Y., Shimizu, R., Haraguchi, M., Naoi, Y.: Polarized emission characteristics of UV-LED with subwavelength grating. Jpn. J. Appl. Phys. **53**, 072101 (2014)
18. Wang, M., Cao, B., C. Wang, C., Xu, F., Lou, Y., Wang, J., Xu, K.: High linearly polarized light emission from InGaN light-emitting diode with multilayer dielectric/metal wire-grid structure. Appl. Phys. Lett. **105**, 151113 (2014)
19. Takashima, Y., Tanabe, M., Haraguchi, M., Naoi, Y.: Highly polarized emission from a GaN-based ultraviolet light-emitting diode using a Si-subwavelength grating on a SiO_2 underlayer. Opt. Commun. **369**, 38-43 (2016)
20. Lalanne, P., Hugonin, J.P., Chavel, P.: Optical properties of deep lamellar gratings: A coupled Bloch-mode insight. J. Lightwave Technol. **24**, 2442-2449 (2006)
21. Magnusson, R., Shokooh-Saremi, M.: Physical basis for wideband resonant reflectors. Opt. Express **16**, 3456-3462 (2008)
22. Karagodsky, V., Sedgwick, F.G., Chang-Hasnain, C.J.: Theoretical analysis of subwavelength high contrast grating reflectors. Opt. Express **18**, 16973-16988 (2010)
23. Ahmed, A., Liscidini, M., Gordon, R.: Design and analysis of high-index-contrast grating using coupled mode theory. IEEE Photonics J. **2**, 884-893 (2010)
24. Karagodsky, V., Pesala, B., Sedgwick, F.G., Chang-Hasnain, C.J.: Dispersion properties of high-contrast grating hollow-core waveguides. Opt. Lett. **35**, 4099-4101 (2010)
25. Rakic, A.D., Djurisic, A.B., Elazar, J.M., Majewski, M.L.: Optical properties of metallic films for vertical-cavity optoelectronic devices. Appl. Opt. **37**, 5271-5283 (1998)

26. Aspnes, D.E., Studna, A.A.: Dielectric functions and optical parameters of Si, Ge, GaP, GaAs, GaSb, InP, InAs, and InSb from 1.5 to 6.0 eV. Phys. Rev. B **27**, 985-1009 (1983)
27. Johnson, P.B., Christy, R.W.: Optical constants of transition metals: Ti, V, Cr, Mn, Fe, Co, Ni, and Pd. Phys. Rev. B **9**, 5056-5070 (1974)
28. Botten, I.C., Graig, M.S., Mcphedran, R.C., Adams, J.L., Andrewartha J.: The dielectric lamellar diffraction grating. Optica Acta 28, 413-428 (1981)

Figure Captions

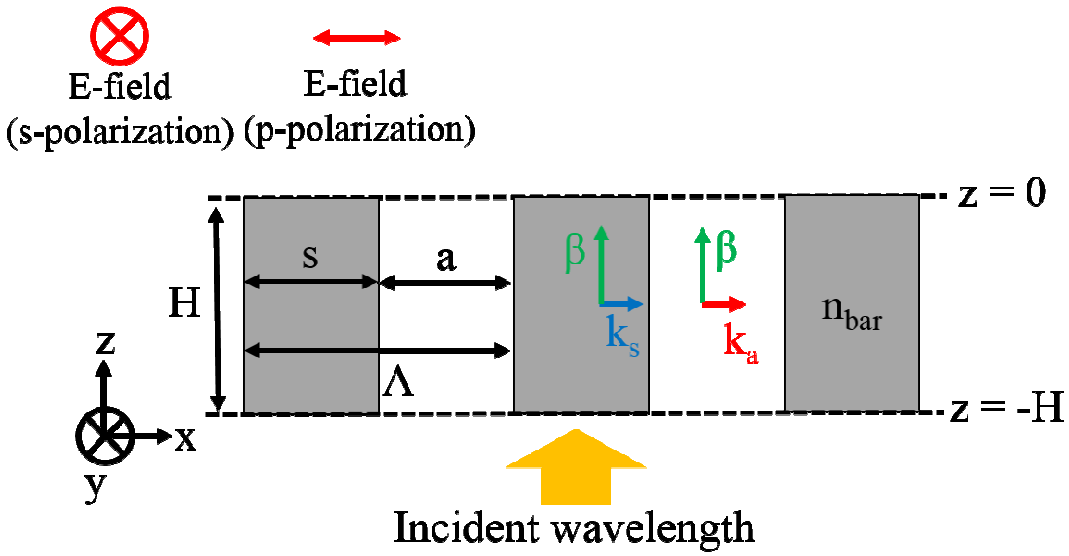

Fig. 1 Cross-sectional view of subwavelength grating (SWG) structure for dispersion analysis. The SWG was arranged in air. The symbols Λ, H, s, a, and n_{bar} indicate the grating period, height, grating width, width of the air gap, and the grating refractive index, respectively. The grating has an infinite length in the y-direction. The grating material was assumed to be Si, Ge, Cr, or Pt. A normal incident plane wave with a 365-nm wavelength was assumed, being p- or s-polarized. The incident light propagated in the z-direction through the SWG.

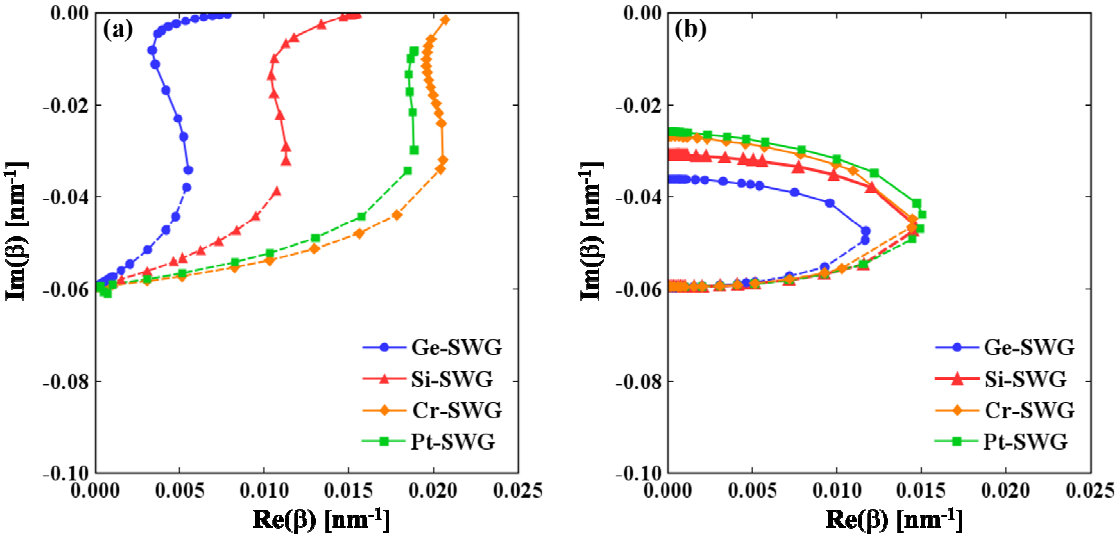

Fig. 2 Real and imaginary parts of propagation constant for (a) p- and (b) s-polarized eigenmodes. The solid and dashed lines correspond to the first- and second-order eigenmodes, respectively

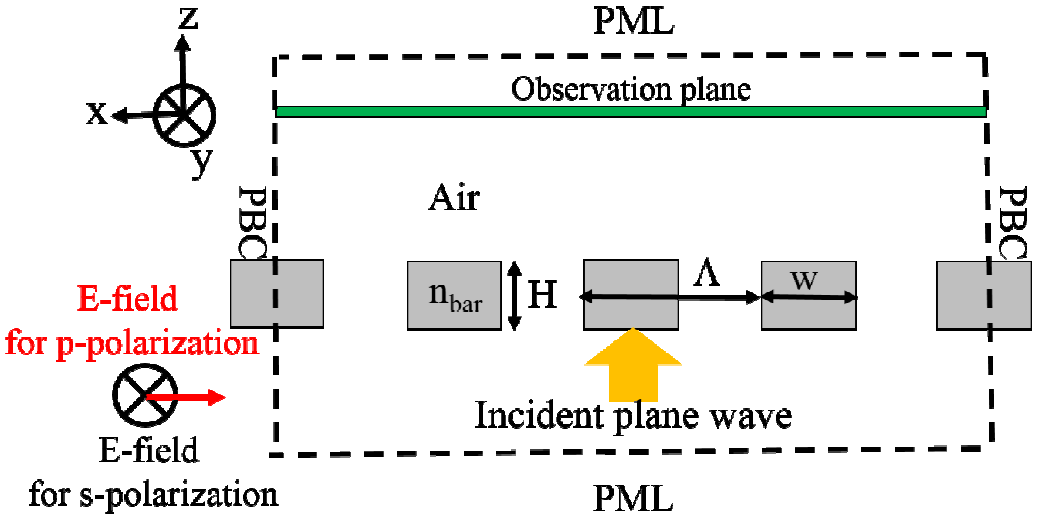

Fig. 3. Schematic of finite difference time domain (FDTD) calculation model. Perfectly matched layers (PMLs) and periodic boundary conditions (PBCs) were employed as the boundary conditions for the *z*- and *x*-directions, respectively. The number of PML layers was 20. The calculation region was defined as a square region surrounded by broken lines, and was divided into a 2 nm × 2 nm rectangular cell. The calculation time step was 3.3×10^{-18} s. The SWG was arranged in air. An incident plane wave with a 365-nm wavelength propagated along the *z*-direction through the SWG.

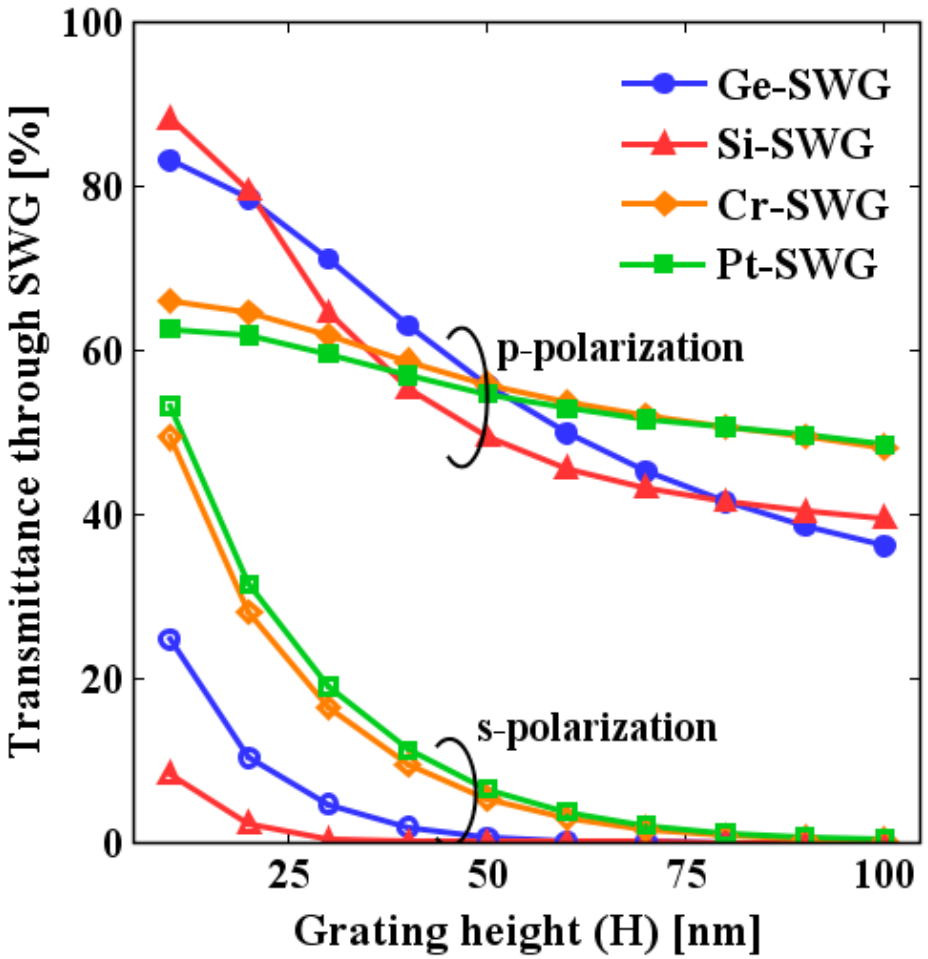

Fig. 4 Calculation of transmittance through SWG as a function of grating height (*H*) using the FDTD method. The filled and open symbols indicate the transmittance of the p- and s-polarization, respectively

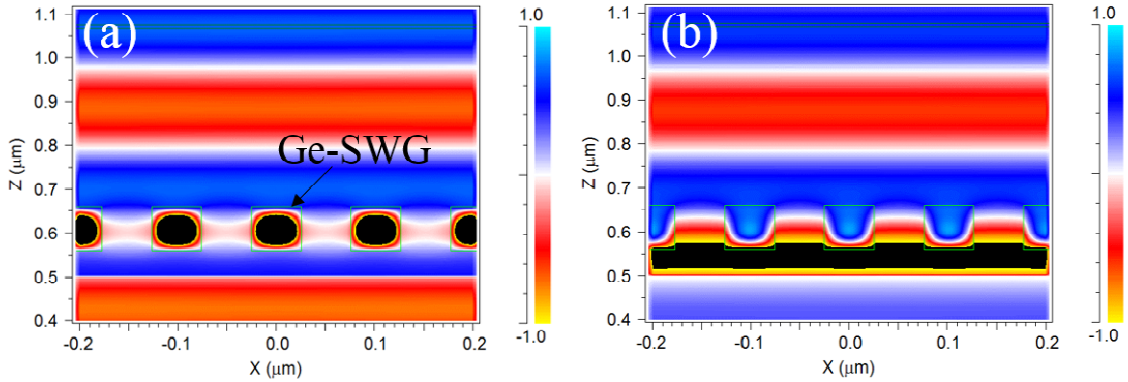

Fig. 5 Magnetic field distribution of p-polarized eigenmode within Ge-SWG, (a) without and (b) with the imaginary part of n_{bar}

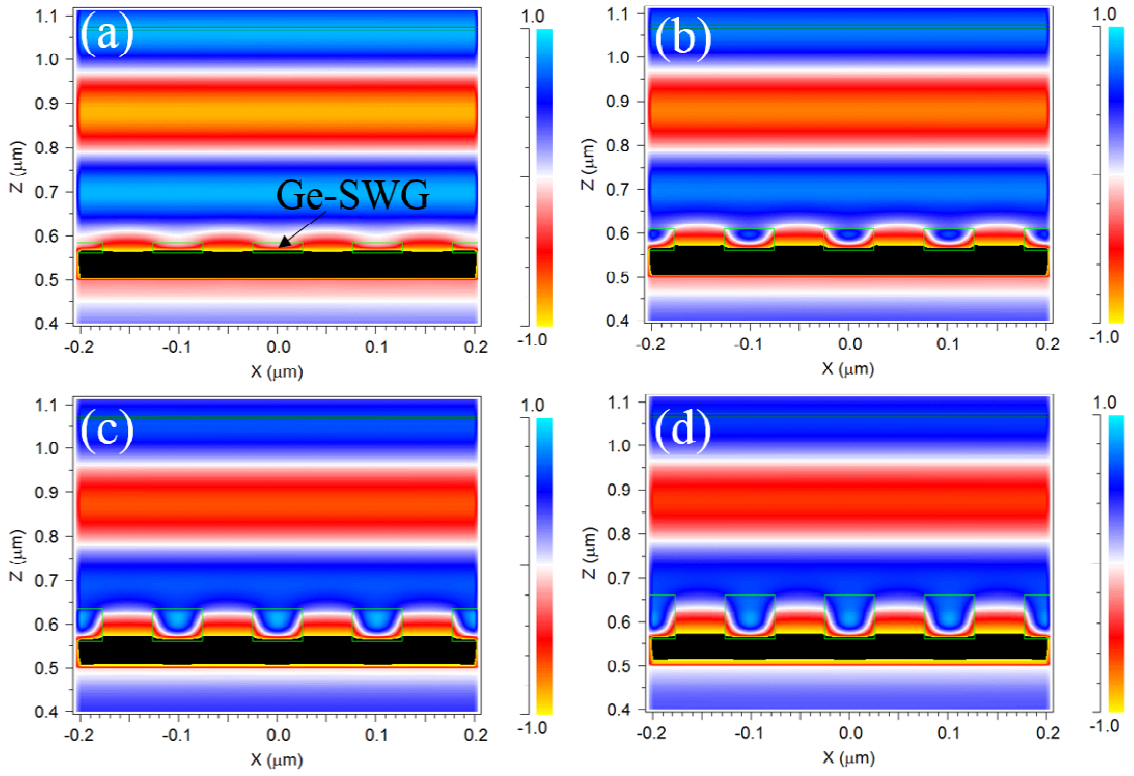

Fig. 6 Dependence of p-polarized eigenmode magnetic field distribution within Ge-SWG on *H*, for *H* = (a) 25, (b) 50, (c) 75, and (d) 100 nm

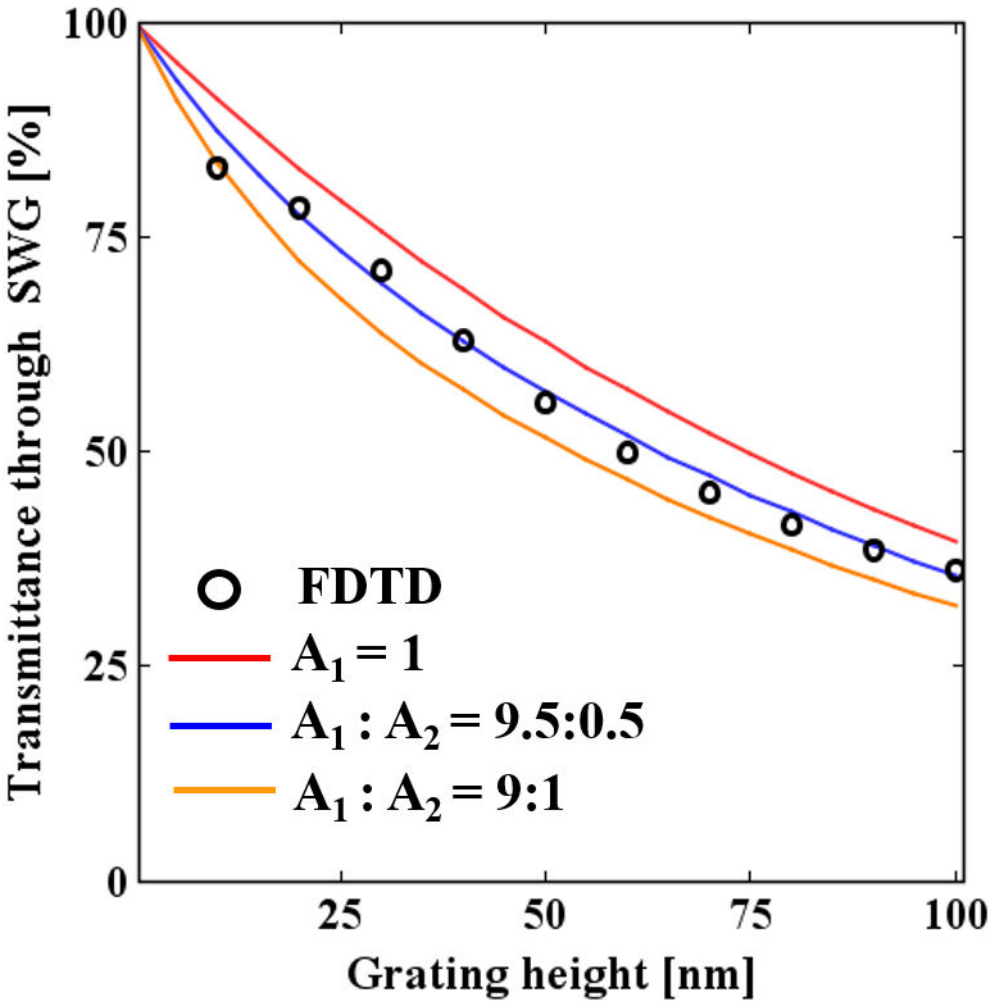

Fig. 7 Dependence of p-polarization transmittance through Ge-SWG as a function of *H* for various first- and second-order mode weights